Immobilization of 99-Technetium (VII) by Fe(II)-Goethite and Limited Reoxidation

Wooyong Um[1,*], Hyunshik Chang[1], Jonathan P. Icenhower[1,§], R. Jeffrey Serne[1], Nikolla P. Qafoku[1], Joseph H. Westsik Jr.[1], Edgar C. Buck[1], Steven C. Smith[1], and Wayne W. Lukens[2]

1 Pacific Northwest National Laboratory

2 Lawrence Berkeley National Laboratory

* Corresponding author: Pacific Northwest National Laboratory, PO Box 999, P7-54, 902 Battelle Boulevard, Richland, WA 99354; wooyong.um@pnl.gov ; phone: (509)372-6227; fax (509)371-7249; § Current address: MS50A4037, Lawrence Berkeley National Laboratory, Berkeley, CA 94720.

To be submitted to ES&T

December, 2010

Abstract

During the nuclear waste vitrification process, some ^{99}Tc is volatilized and is trapped by melter off gas scrubber solutions, and plans are currently being contemplated for the disposal of such secondary waste. Solutions containing pertechnetate [$^{99}Tc(VII)O_4^-$] were mixed with precipitated goethite and dissolved Fe(II) to determine if an iron (oxy)hydroxide-based waste form can reduce technetium and isolate Tc(IV) from oxygen. The results of these experiments demonstrate that Fe(II) with goethite efficiently catalyzes the reduction of Tc(VII) to Tc(IV) from simple (deionized water) to complex solutions mimicking the chemical composition of caustic waste scrubber media. Analyses of the resultant Tc-bearing solid products by XAFS indicate that all of the Tc(VII) was reduced to Tc(IV) and that the latter is incorporated as octahedral Tc(IV), which is consistent with direct substitution of Tc(IV) for Fe(III) in the goethite or magnetite structure. Batch dissolution experiments, conducted under ambient oxidizing conditions for more than 180 days, demonstrated a very slow release of Tc to solution, consistent with the incorporation of Tc(IV) into the stable goethite lattice. Incorporation of Tc(IV) into the goethite lattice thus provides significant advantages for curtailing release and limiting reoxidation of Tc disposed in nuclear waste repositories.

Introduction

Technetium is generated in large quantities as a fission product by the irradiation of ^{235}U-enriched fuel during production of commercial power and nuclear weapons. The most abundant Tc isotope in the wastes, ^{99}Tc, has a high fission yield (~6%) and a long half-life (2.13×10^5 years) [1, 2]. During the Cold War era, generation of fissile ^{239}Pu for use in atomic weapons yielded nearly 1900 kg of ^{99}Tc at the Hanford Site, USA [3]. Most of this Tc is present in fuel reprocessing wastes currently stored in underground tanks awaiting retrieval and permanent disposal. After retrieval, the wastes will be separated into high- and low-activity streams, which will be vitrified and disposed of separately. Even with careful process controls, volatilization of some Tc during the vitrification of the wastes is expected. Although most of the volatilized Tc will be captured in melter off-gas scrubbers and returned to the melter, a portion of the Tc is expected to become part of the secondary waste stream. Effective and cost-efficient disposal of the Tc in the off-gas scrubber solution is projected to be difficult.

A number of waste forms aimed at immobilizing Tc have been proposed and have merit [4 – 6]. Yet any strategy to immobilize Tc for ~ 2 million years (10 half-lives) must account for the reactivity of the waste form in the disposal environment and the propensity for aqueous Tc(VII) to migrate in the subsurface without retardation. A component of past strategies has been to use reducing agents to transform Tc(VII) into the less mobile Tc(IV) species. When manifested as the hydrated oxide ($TcO_2\bullet nH2O$), sulfide (TcS_2), or as a co-precipitate with iron (oxy)hydroxides, the solubility and mobility of technetium is very low. However, Tc(IV) in the form of the hydrated oxide has the potential to re-oxidize rapidly to Tc(VII) upon contact with oxygen [4, 5].

Therefore, developing a chemically inert waste form that minimizes contact between reduced Tc(IV) and oxygen is key to the success of any proposed immobilization strategy.

Iron oxides, hydroxides, and (oxy)hydroxides are the end-stage weathering products of a wide range of natural and anthropogenic materials, and among these, goethite [α-Fe(III)O(OH)] is the most thermodynamically stable phase over a range of particle size and moisture conditions [6]. The stability of goethite at or near Earth's surface and its resistance to change in isotopic composition during low temperature geochemical processes has led to the use of goethite as an indicator of paleotemperatures [7, 8]. Previous investigations have also revealed that when Tc is incorporated into less stable iron phases, the transformation into goethite occurred without oxidation or release of Tc to solution [9, 10]. Additional studies have shown that the oxidized form of technetium, pertechnetate [TcO_4^-], is reduced in the presence of Fe(II), but the form of the ferrous iron, and the identity of the phase with which it is associated, matters greatly [9-11]. When Fe(II) is sorbed onto an iron-bearing solid, pertechnetate is reduced more rapidly compared to when Fe(II) is present as a structural cation in silicate minerals, sorbed onto clays or other silicates, or when ferrous iron is dissolved in solution [9, 11-13]. It may also be possible to directly substitute Tc(IV) for Fe(III) in the octahedral site of goethite during precipitation and crystal growth reactions because of the similarity in ionic radii [78.5 Å for both Fe(III) and Tc(IV)] and the interatomic distances between Fe(III)—O and Tc(IV)—O (2.06 and 2.01 Å, respectively) [14]. The substitution of Tc(IV) for Fe(III) must be charge balanced, which could occur by either replacement of an Fe(III) ion by an Fe(II) ion, as in the case of ulvospinel (Fe_2TiO_4), or by the generation

of vacancies on the Fe(III) sites as in the case of maghemite (γ-Fe_2O_3) or Sn(IV) substituted goethite. (refs: Amer. Miner, 2010, 95, 425-439; J Mater Chem, 2000, 10, 1643-1648. I am unaware of any cases of charge balance in iron oxides produced by additional oxide or hydroxide ions – Wayne). Therefore, a waste form based on a Fe(II)-goethite system is an attractive candidate for deposition of technetium from secondary wastes.

The experiments described herein evaluate immobilization of Tc in Fe(II)-goethite system and attempt to elucidate the local structure of Tc within the final Tc-goethite product. In addition, the release potential of Tc from the Tc-goethite waste form was evaluated using batch dissolution experiments in a variety of aqueous solutions.

Experimental Section

Solution Preparation. Pertechnetate solutions were prepared by adding sodium pertechnetate stock solution to the following solutions; deionized water (DIW), a synthetic scrubber solution (SSS-1) made by mixing predominately ammonium carbonate and sodium hydroxide to DIW and another synthetic scrubber solution (SSS-2) made by mixing predominately sodium forms of hydroxide, nitrate, aluminate and oxalate salts. Other components present in these two SSS simulants are listed in Table 1. The concentration of pertechnetate in the DIW and SSS solutions ranged from 2.2×10^{-5} M to 4.2×10^{-4} M.

Goethite Synthesis Steps and Strategy for Tc(VII) Removal. Goethite was synthesized based on a scaled-down procedure of Schwertmann and Cornell [15]; details can be found in the Supporting Information (SI). Between 2.75 and 3.50 g of synthesized

110 goethite dry powder was resuspended in 250 mL of deaerated deionized (DDI) water in
111 an anoxic chamber (Coy Laboratory) equipped with a H_2/O_2 gas analyzer, palladium
112 coated alumina catalyst, and a mixture of N_2 (96%) and H_2 (4%) gas. The initial pH of
113 the goethite slurry was 10.4 and it was adjusted to pH ~ 2.0 with 2 M HNO_3. An aliquot
114 of $FeCl_2 \cdot 4H_2O$ (3.48 g) was directly added to the goethite slurry to make 0.07 M of
115 dissolved Fe(II), while the suspension was continuously stirred at low pH (~2.0) in the
116 anoxic chamber. (After 1 day of stirring, 0.25 mL of Tc(VII) from a $NaTcO_4$ standard
117 solution was added to produce 2.2×10^{-5} M Tc in the Fe(II)-goethite slurry. As soon as the
118 Tc(VII) was added, the bottle was immediately capped and mixed before subsampling for
119 total Tc concentration in the supernate. After subsampling, 150 mL of 2 M sodium
120 hydroxide (NaOH) was added, and an additional subsample was immediately collected.
121 The final slurry was placed in an oven at 80^{o}C for 7 days to promote additional
122 precipitation of a Tc-goethite solid.) – Was this done in the anaerobic chamber or in air?
123 If this was done in an anaerobic chamber, magnetite will be stable under the reaction
124 conditions. After 7 days, the final Tc-goethite solids were separated by filtration, washed
125 using DI water, air dried, and set aside for additional analysis.
126 In select experiments, the Tc-goethite solids were modified to armor the Tc-
127 goethite solids with additional goethite using separately prepared $Fe(NO_3)_3 \cdot 9H_2O$
128 (11.4g/100 mL) and 2 M NaOH (150 mL) solutions in air. These two solutions were
129 added sequentially right after the Tc-goethite slurry was mixed with an initial 2 M NaOH.
130 After 1 to 2 days of reaction with the ferric nitrate and sodium hydroxide solutions, the
131 bottle containing the final slurry was placed inside an oven at 80^{o}C for 7 days. The final
132 slurry was subsequently filtered, and both the solution and solid samples were subjected

133 to further analyses. For Sample 2-5, the order of adding the ferric nitrate and sodium
134 hydroxide was reversed such that NaOH was added before the $Fe(NO_3)_3 \cdot 9H_2O$ was
135 introduced. One sample, 2-3* was prepared with higher total Tc(VII) concentration
136 (4.2×10^{-4} M) and 0.1 M of Fe(II) in the SSS-2. The various goethite synthesis products
137 are given in Table 2.

138 The synopsis given in Table 2 indicates that samples 2, 2-1, 2-2, and 2-5 were Tc-
139 goethite solids generated using Tc(VII)-spiked DIW and 2-3, 2-3* and 2-4 were generated
140 using Tc(VII)-spiked synthetic scrubber solutions (SSS-1 or SSS-2). Samples 2-2, 2-3,
141 and 2-3* had no further Fe(III) armoring performed, whereas Samples 2, 2-1, 2-4, and 2-5
142 were subjected to additional Fe(III) armoring.

143 **Solution Analysis**. At each sub-sampling step over the course of each Tc
144 sequestering experiment, a small aliquot of filtered solution was set aside for
145 determination of pH and the concentrations of Tc, Fe(II), and total Fe (Fe_{Tot}).
146 Concentrations of Tc and Fe_{Tot} in the supernatants were measured using ICP-MS and
147 ICP-OES, respectively. The dissolved ferrous [Fe(II)] concentration was determined
148 using the ferrozine colorimetric method [16].

149 **Solid Phase Characterization.** The initial goethite substrate and the final solid
150 product were characterized using X-ray diffraction (XRD), scanning electron microscopy
151 (SEM), and transmission electron microscopy (TEM) with energy dispersive x-ray
152 (EDX) spectroscopy. Details of these solid phase analyses are included in the SI and
153 described in Um et al. (2010) [17]. An acid extraction procedure using 8 M HNO_3 at
154 90°C and ICP-MS analysis were used to determine the total Tc(VII) concentration in the
155 final Tc-goethite solid.

Tc-Goethite Dissolution Experiments. Batch-leaching experiments were conducted using a powder of Sample 2 at 1 g L^{-1} in different leaching solutions. The contacting solutions were of three types. The first three solutions were standard Beckman-Coulter® pH buffer solutions at pH 4 (potassium hydrogen phthalate), pH 7 (mixture of potassium and sodium dihyrogen phosphate), and pH 10 (mixture of sodium bicarbonate-carbonate). The second type of solution was a synthetic pore water (pH=7.2 and ionic strength=0.05 M) simulating a composition anticipated from the Integrated Disposal Facility (IDF) in the Hanford 200 East Area[18]. The third solution was a simulated Waste Treatment Plant (WTP) glass leachate (GL) with pH=9.7 and an ionic strength of 1.67 M [18, 19]. The chemicals used to prepare the latter two Hanford-specific leaching solutions are shown in Table SI-1. Additional Tc-goethite powder samples (Sample 2-5; with armoring) and (Sample 2-2; without armoring) were reacted using only the simulated IDF pore water solution to investigate the effect of the armoring process on Tc release. For each Tc-goethite dissolution test, a supernate subsample (1 mL) was periodically collected, filtered with a 0.45-μm Nalgene syringe filter, and submitted for analyses of Fe(tot) and Tc. The pH was directly measured in the slurry solution after subsampling. After the 180-day dissolution tests were completed, the powder Tc-goethite samples were separated by filtration and subjected to solids characterization.

X-ray Absorption Fine Structure (XAFS) Spectroscopy. Solid technetium standards and Tc-goethite samples (2, 2-2, 2-3*, and 2-5) before they were subjected to dissolution tests were analyzed to determine the Tc oxidation state and Tc local structure using x-ray absorption near edge structure (XANES) and extended x-ray absorption fine

179 structure (EXAFS) spectroscopy, respectively. The Tc-goethite Samples 2, 2-2, and 2-5
180 were reanalyzed after being contacted with solution for 180 days to determine the final
181 Tc oxidation state. An additional aliquot of the Tc-goethite Sample 2 was separately
182 exposed to atmospheric oxygen for 180 days and the Tc oxidation state in this sample
183 was also determined.

184 The XAFS spectra were collected either on beamline X10C at the National
185 Synchrotron Light Source (NSLS) or on beamline 4-1 at the Stanford Synchrotron
186 Radiation Laboratory (SSRL). Data reduction and analysis were performed using the
187 software IFEFFIT [20] and ATHENA/ARTEMIS [21] after correction for detector dead-
188 time. The XANES spectra for the Tc-goethite samples were fit using a linear
189 combination of the XANES spectra of Tc(IV) and Tc(VII) standards[22]. Three different
190 models were tested for EXAFS data: (Model 1) Tc substituted for Fe in the goethite
191 structure without any neighboring Tc atoms, (Model 2) Tc substituted for Fe in the
192 goethite structure with a small fraction of neighboring Fe sites occupied by Tc, and
193 (Model 3) Tc substituted for Fe in the goethite structure with some Tc present as separate
194 $TcO_2 \cdot 2H_2O$ precipitates. More details for XAFS sample collection and analysis are given
195 in the SI.
196

197 Results and Discussion

198 **Tc(VII) Removal by Fe(II)-Goethite.** The total amount of Tc measured in the final Tc-
199 goethite solid indicated that 93 to 100% of the Tc from the DIW solution and 93 to 96%
200 of the Tc from the synthetic scrubber solutions was removed (Table 2). The greatest Tc
201 removal, 100%, was found in Sample 2-5 (Table 2), which was prepared by the addition

202 of NaOH prior to the armoring Fe(III). In Sample 2-5, most of the dissolved Fe(II) and
203 Tc(VII) added to the goethite suspension precipitated immediately upon adding the
204 NaOH, prior to adding the Fe(III) armoring solution (Figure SI-1d). Similar rapid and
205 effective removal of Tc was also observed in Samples 2-2 and 2-3 prepared with DIW
206 and the SSS-1 (pH~13), respectively, even without the additional Fe(III) armoring
207 process (Figure SI-1b and 1c). Sample 2-3 prepared with highly caustic SSS-1 showed
208 almost 100% Tc removal in solution before addition of NaOH because of initially high
209 pH of SSS-1 (Table 2 and Figure SI-1c). This suggests that the key step in Tc removal is
210 making the mixture alkaline after mixing Tc with the Fe(II)-goethite slurry prepared at
211 low pH. In addition, 100% of Tc removal observed in Sample 2-5 was found to occur
212 after adding NaOH but before adding additional Fe(III), indicating that the amount of
213 additional Tc removed from solution during the Fe(III) armoring process was not
214 significant (Figure SI-1d). The mass balance of total Fe used to create the Tc-goethite
215 samples also showed that about 90% to100% of total Fe used in this system was
216 recovered from the final Tc-goethite product (Figure SI-2).

217 **Solid Phase Characterization**. The XRD pattern of the initial goethite solid
218 showed only goethite in the sample (Figure 1). However, goethite was not the only
219 crystalline phase observed in the final Tc-goethite products, and also included noticeable
220 amounts of magnetite (arrows in Figure 1) in Samples 2, 2-1, 2-2, 2-3, and 2-3* as
221 indicated by the sharp peak at 35.6 degrees 2-theta. This peak was more discernable in
222 Samples 2-2, 2-3, and 2-3*, which were prepared without additional Fe(III) armoring.
223 Samples 2-2 and 2-3 were dark greenish-black and contained more fine particles that
224 were attracted to the magnetic stir bar indicative of the presence of a magnetic species

225 (i.e., magnetite). Semiquantitative analysis using standard magnetite and goethite XRD
226 patterns showed approximately 70% and 60% magnetite content for Samples 2-2 and 2-3,
227 respectively, with the remainder being goethite (Figure SI-3). A smaller amount of
228 magnetite, 20% and 40%, was found in Sample 2-3* and 2, respectively. Two possible
229 explanations for the formation of magnetite are 1) the initial precipitation of ferrous
230 hydroxide, $Fe(OH)_{2(s)}$ and its gentle oxidation to magnetite by nitrate as pH increased (ref
231 Mat Res Bull 2006, 41, 703) or 2) the reaction with dissolved Fe(III) in the initial Fe(II)
232 goethite slurry at low pH.(ref Mat Res Bull 2006, 41, 703) More details for this
233 explanation can be also found in the SI.
234 The XRD peak at 21 degrees 2-theta region, indicative of the presence of goethite,
235 were more intense in the Samples 2-4 and 2-5, prepared with additional Fe(III) armoring,
236 than in Samples 2-2 and 2-3, which were prepared without additional Fe(III) (Figure 1).
237 No major magnetite was found in Samples 2-4 and 2-5. In addition, no siderite ($FeCO_3$)
238 was found in Samples 2-3 and 2-4 even though synthetic off-gas scrubber solution
239 contained 0.8 M carbonate (Figure 1).
240 The goethite phase also showed no alteration upon leaching. The final Tc-goethite
241 samples after 180 days of leaching showed identical XRD patterns to the initial Tc-
242 goethite samples (Figure SI-5). No mineralogical change was observed in those leached
243 Tc-goethite samples, even for the final Tc-goethite Sample 2, which had been leached in
244 a pH=10 buffer solution for 180 days and showed the highest dissolved Fe(tot)
245 concentration (See below leaching results).
246 The SEM images of both the initial and final Tc-goethite products exhibited the
247 acicular shape typical of goethite (Figure 2). Small cubes or pseudocubic crystals, likely

248 magnetite, attached to acicular goethite were observed in Samples 2-2, 2-3, and 2-3*,
249 which is consistent with the observation of magnetite found in these samples by XRD
250 analysis. However, no cubic-shaped crystals were found in Sample 2-5 (Figure 2c).
251 Additional TEM results revealed similar acicular goethite in Samples 2-2 and 2-3 with
252 the selected area electron diffraction (SAED) pattern taken along the **B**[001] direction of
253 goethite (Figure 3).
254 Because Samples 2-2 and 2-3 contained a relatively higher Tc concentration per gram
255 of goethite (Table 2), Tc could be detected in Sample 2-2 by TEM/EDX (Figure 3d).
256 However, the exact location of Tc was not clear because the Tc EDX peak was found in
257 the mixture of magnetite and goethite in Sample 2-2. The presence of Tc was observed
258 by TEM/EDX in an acicular-shaped particle (goethite) in Sample 2-3*, which was
259 prepared with high Tc concentration (Figure 3e). However, Tc was also detected by
260 SEM/EDX for the same Sample 2-3* in a separated mineral particle that had the typical
261 cubic shape of magnetite (Figure 2d and 2e). The presence of Tc in the final Tc-goethite
262 product in Sample 2-2 and 2-3* indicates the possibility that Tc is associated with Fe
263 oxide, either magnetite or goethite.
264 **Tc Release in Batch Dissolution Experiments.** Batch-leaching data for Sample 2
265 as a function of time in different solutions are shown in Figure 4. No dramatic changes
266 of measured pH values were observed (Figure 4c). Concentrations of Tc in the leachates,
267 even after 180 days of contact, were less than 2 μg/L (2×10^{-8} M) in the pH = 4 and 7
268 buffer solutions and the IDF pore water (pH = 7.2) solutions. These solution
269 concentrations equate to a Tc release of ~2 μg Tc/g of Tc-goethite solid. The release of
270 Tc was higher when the Tc-goethite solids were immersed in the pH = 10 buffer (up to 7

μg Tc/g of Tc-goethite solid) and GL solutions (up to 2.7 μg Tc/g of Tc-goethite solid) (Figure 4a). The leached Tc concentrations in the IDF pore water and pH = 7 buffer solution were very similar, and most of the measured Fe(tot) concentrations in these solutions were below the detection limit (< 50 μg/L) of ICP-OES, which is not surprising since the goethite solubility is $<10^{-11.9}$ M at pH 7 [23]. (I have converted Schwertmann's concentration to molarity. The solubility product is -0.02, but would need to be defined as it can be written using the concentration of either protons or hydroxide). Because the GL solution has a relatively high pH (~9.7) compared to the IDF pore water, more goethite dissolved resulting in higher leached Tc concentrations in GL solution than the IDF pore water solution. A progressively increasing dissolved Fe(tot) concentration after 180 days of reaction time was found only for the pH = 10 buffer solution and indicates that Tc release occurs mainly as the host magnetite and/or goethite dissolves. A linear relation between dissolved total Fe and released total Tc concentrations was also observed in the pH = 10 solution (Figure SI-5).

Additional Tc leaching tests using powdered Tc-goethite Samples 2-2 and 2-5 in IDF pore water solution were conducted to investigate the effect of the goethite armoring process. The results of these additional leach tests on armored (Samples 2 and 2-5) and unarmored (Sample 2-2) powder samples showed no detectable Fe(tot) in the IDF pore-water leachates for all three Tc-goethite samples even after 180 days of leaching as found for Samples 2 in Figure 4b. Especially at early leaching times of less than 10 days (Figure 4d), noticeably more Tc was leached from Sample 2-2, which was prepared without additional goethite armoring and consisted 70% magnetite, compared to Samples 2 and 2-5 that were prepared with two different armoring processes and in which goethite

294 is the dominant mineral phase. Although Samples 2 and 2-5 were both prepared with
295 additional goethite armoring, Sample 2-5 (100% goethite) showed complete Tc removal
296 from solution (100% Tc uptake in Table 1) and was the most resistant to Tc leaching (less
297 than 2.0 wt% of Tc removed after 180 days in IDF pore water).

298 **XAFS Analysis of Tc in Tc-Goethite.** The XANES spectra for the Tc standards
299 $KTcO_4$, $NaTcO_4$, TcO_4^- adsorbed on Reillex-HPQ resin, and $TcO_2 \cdot 2H_2O$, along with the
300 Tc-goethite Samples 2, 2-2, 2-3*, and 2-5, are shown in Figure 5. The spectra for
301 $NaTcO_4$, $KTcO_4$, and TcO_4^- adsorbed on ion-exchange resin are very similar and
302 characterized by a strong pre-edge feature due to the 1s to 4d transition, which is allowed
303 for the tetrahedral TcO_4^- anion. The XANES spectrum of $TcO_2 \cdot 2H_2O$ is very different
304 and characteristic of Tc(IV) coordinated by 6 oxygen atoms in an octahedral geometry.
305 In addition, the absorption edge of $TcO_2 \cdot 2H_2O$ is 5.5 eV lower in energy than the
306 absorption edge of TcO_4^-. The oxidation state of Tc in the Tc-goethite samples was
307 determined by fitting their XANES spectra using the spectra of TcO_4^- adsorbed on
308 Reillex-HPQ resin and $TcO_2 \cdot 2H_2O$ as the Tc standards (Figure 5). In all cases, the results
309 of fitting indicated that only Tc(IV) was present in Samples 2, 2-2, 2-3*, and 2-5 before
310 leaching (Figure 5a). The uncertainty in the amount of TcO_4^- present varied from 2-3%,
311 which gives a detection limit of 5% at the 95% confidence level.

312 The oxidation state of Tc in the leached Tc-goethite samples was also determined by
313 fitting their XANES spectra using the Tc standards and the results indicated that only
314 Tc(IV) was present in Samples 2, 2-2, and 2-5, even after 180 days reaction in IDF
315 solution (Figure 5b). The Tc-goethite Sample 2 that was exposed to atmospheric oxygen
316 for 180 days also showed only that the Tc(IV) oxidation state was present (Figure 5b).

Other Tc-goethite samples that were leached in different pH solutions also showed no reoxidized Tc(VII) in the XANES spectrum (Figure SI-6). The fraction of Tc present as TcO_4^- in all the reacted Tc-goethite samples in solution or air for 180 days was less than 5%, suggesting that Tc(IV) incorporated within the goethite mineral lattice is resistant to reoxidation.

The k^3-weighted EXAFS spectra and Fourier Transforms for Samples 2, 2-2, 2-3*, and 2-5 solids before leaching are presented in Figure (SI-8). The figure is missing and I assume you have placed it in the SI. The numerical fitting results are in Table 3. As described in previous section, three different models were examined and the distances were allowed to vary in fitting process. Therefore, if the distances to neighboring atoms did not correspond to the model, the structure was free to relax.

In all cases, the local environment of Tc is consistent with Tc replacing Fe in the goethite lattice. This is best illustrated by comparing the Tc local environment to the Fe environment in "pure" goethite, which is also presented in Table 3. The main difference between the local environment of Tc in the Tc-goethite and that of Fe in "pure" goethite is that in "pure" goethite, there are two sets of two iron atoms at 3.01 and 3.28 Å, while in the structure determined by EXAFS for the Tc-goethite solids, there are four iron atoms at an intermediate distance, 3.1 Å. This difference could be either an inability to resolve the two sets of iron neighbors in the EXAFS analysis of the Tc-goethite solids or could be due to disorder in the local environment of Tc-goethite caused by the Tc substituting for Fe. Unlike the other samples, Sample 2 also displays additional scattering due to a Tc neighbor at 2.51 Å, which is not consistent with a neighboring Tc in the goethite lattice. This distance, however, is consistent with the presence of

340 $TcO_2 \cdot 2H_2O$, which has a solubility of $5x10^{-8}$ M at pH=2.0 [24], and is attributed to the
341 presence of residual Tc(IV) not incorporated into the goethite lattice in Sample 2.
342 A similar local environment for Tc in iron oxides was observed previously in TcO_4^-
343 reduced using green rust [10]. In that case, the initial Tc environment was consistent
344 with Tc incorporated into the lattice of green rust. And after the green rust was oxidized,
345 the coordination environment was consistent with Tc substituted for Fe in goethite
346 produced by oxidation of the green rust. The Tc-Fe distances in the oxidized products are
347 very similar to those determined here, although the previously reported Tc-Fe
348 coordination numbers for the oxidized green rust and goethite [10] are smaller than those
349 reported here.
350 The local environment of Tc in goethite is distinctly different from that of Tc
351 adsorbed on the surfaces of iron oxides. Peretyazhko et al. (2009) [25] examined Tc(IV)
352 adsorbed on both goethite and hematite. In both cases, a complex coordination geometry
353 was observed with a first shell consisting of six oxygen atoms at 2 Å, a neighboring metal
354 atom (either Tc or Fe) at 2.6 A, three oxygen atoms at 3 Å, and two iron atoms at 3.5 Å.
355 A similar local environment was also observed for Tc adsorbed on ferrihydrite [9]. In
356 comparison to these previous reports, it is unlikely that Tc in our Tc-goethite samples is
357 adsorbed onto the iron oxide mineral surfaces.
358 While the local environment of Tc in our Tc-goethite is distinctly different from Tc
359 adsorbed onto the surface of iron oxides, it is not necessarily distinct from Tc
360 incorporated into other iron oxides. The distances of Tc to neighboring atoms in Tc-
361 goethite are similar to those of the octahedral site in magnetite: six oxygen atoms at
362 2.06 Å, six iron atoms at 2.97 Å, and six iron atoms at 3.48 Å. Although it may be

363 possible to distinguish these two possibilities using the numbers of neighboring iron
364 atoms, this is not done here because coordination numbers determined by EXAFS are not
365 particularly accurate and can be lower than expected if some portion of the Tc is
366 adsorbed on the surface rather than incorporated into the lattice. However, in the case of
367 the Tc-goethite samples, especially Samples 2 and 2-5 which were prepared with
368 additional armoring, assignment of Tc in the final Tc-goethite product rather than
369 magnetite is made for the following reasons. First, the Tc-Fe distances in the samples
370 examined here are all similar and somewhat longer than those of the octahedral magnetite
371 site and are more similar to the goethite model. Second, goethite is a major mineral
372 found in those samples (Figure 1). However, because magnetite is a major phase (60% to
373 70%) in Samples 2-2 and 2-3 (Figure SI-3) and magnetite can be transformed to goethite
374 by additional armoring process in alkaline condition [26], the possibility of initial
375 removal of Tc by magnetite, which is subsequently transformed to goethite cannot be
376 ruled out. Even though the EXAFS results of Samples 2 and 2-5 are very similar to those
377 found in Samples 2-2 and 2-3* where magnetite and goethite mixture are found,
378 SEM/TEM with EDX analysis for Tc location in Sample 2-3* prepared with high Tc
379 concentration and SSS-2 without the additional armoring process show that Tc can be
380 associated with both magnetite (Figure 2) and goethite (Figure 3). However, the EXAFS
381 result for Sample 2-5 (100% goethite based on XRD analysis) confirmed almost total Tc
382 coprecipitation within the goethite lattice rather than showing Tc adsorbed onto the
383 surfaces of goethite or Tc as a discrete $TcO_2 \cdot 2H_2O$ solid phase. Finding only Tc
384 coprecipitation within goethite lattices in Sample 2-5 is consistent with the Tc leaching
385 results for Sample 2-5 in IDF pore water (Figure 4d) that shows the least Tc release.

Environmental Implications of Tc Incorporated within Goethite. The observed high-percentage Tc incorporation within the Fe(II)-treated Fe oxide mineral (magnetite or goethite) structure provides a viable option for treating waste streams containing Tc(VII) and forming stable Tc-bearing solid waste forms. With Fe(II) acting as a reductant on the surface of initially prepared goethite to reduce Tc(VII), the process can remove Tc from off-gas secondary waste solutions quickly and efficiently. Because goethite is very stable with respect to other iron oxides or (oxy)hydroxides, Tc reduced and incorporated within the goethite is unlikely to be released, even when the final Tc-goethite product is exposed to oxidizing conditions. The sequestered Tc within goethite lattice resists to reoxidation and exhibits lower leachability compared to the literature data [4] on the Tc leachability or release of Tc adsorbed onto ferric oxides or from discrete $TcO_2 \cdot 2H_2O_{(s)}$ crystals present in mixed solids.

Acknowledgments. Funding was provided by the DOE Environmental Management (EM-31) program. Part of this work (TEM analysis) was performed at the W.R. Wiley Environmental Molecular Science Laboratory in PNNL. The authors appreciate Dodge Cleveland for Tc XAFS sample collection in BNL. The PNNL is operated for the DOE by Battelle Memorial Institute under Contract DE-AC05-76RL0 1830. Portion of this research was carried out at the SSRL, a national user facility operated by Stanford University on behalf of the US DOE. Part of this research was performed at Lawrence Berkeley National Laboratory and was supported by the Director, Office of Science, Office of Basic Energy Sciences, Chemical Sciences, Geosciences, and Biosciences

Division, of the U.S. Department of Energy and by the Director, Office of Science, of the U.S. Department of Energy under Contract No. DE-AC02-05CH11231.

Supporting Information. Supporting information includes details of the characterization methods (XRD, SEM, and TEM) and analysis of XAFS, Tc and Fe concentration changes in solution, Fe mass balance in samples, composition of IDF/GL leaching solutions, and SEM/XRD/XANES results. This information is available free of charge via the Internet at http://pubs.acs.org.

418 **References**

419 1. Kotegov, K. V.; Pavlov, O. N.; Shvedov, V. P., *Technetium*. Academic Press:
420 New York, 1968; Vol. 2.
421 2. Luykx, F., Technetium Discharges in the Environment. In *Technetium in the*
422 *Environment*, Desmet, G.; Myttenaere, C., Eds. Elsevier: Essex, UK, 1986.
423 3. Darab, J. G.; Smith, P. A., Chemistry of technetium and rhenium species during
424 low-level radioactive waste vitrification. *Chem. Mat.* **1996,** *9*, 1004-1021.
425 4. Lukens, W. W.; Bucher, J. J.; Shuh, D. K.; Edelstein, N. M., Evolution of
426 Technetium speciation in reducing grout. *Environ. Sci. Technol.* **2005,** *39*, 8064-8070.
427 5. Fredrickson, J. K.; Zachara, J. M.; Plymale, A. E.; Heald, S. C.; McKinley, J. P.;
428 Kennedy, D. W.; Liu, C.; Nachimuthu, P., Oxidative dissolution potential of biogenic and
429 abiogenic TcO_2 in subsurface sediments. *Geochim. Cosmochim. Acta* **2009,** *73*, 2299-
430 2313.
431 6. Navrotsky, A.; Mazeina, L.; Majzlan, J., Size-driven structural and
432 thermodynamic complexity in iron oxides. *Science* **2008,** *319*, 1635-1638.
433 7. Zheng, Y. F., Oxygen isotope fractionation between hydroxide minerals and
434 water. *Phys. Chem. Mineral.* **1998,** *25*, 213-221.
435 8. Yapp, C. P., Oxygen and hydrogen isotope variation among goethite (alpha-
436 FeOOH) and the determination of paleotemperatures. *Geochim. Cosmochim. Acta* **1987,**
437 *51*, 355-364.
438 9. Zachara, J. M.; Heald, S. M.; Jeon, B.-H.; Kukkadapu, R. K.; Liu, C.; Mckinley,
439 J. P.; Dohnalkova, A. C.; Moore, D. A., Reduction of pertechnetate [Tc(VII)] by aqueous
440 Fe(II) and the nature of the solid phase redox products. *Geochim. Cosmochim. Acta* **2007,**
441 *71*, 2137-2157.
442 10. Pepper, S. E.; Bunker, D. J.; Bryan, N. D.; Livens, F. R.; Charnock, J. M.;
443 Pattrick, R. A. D.; Collison, D., Treatment of radioactive wastes: An X-ray absorption
444 spectroscopy study of the reaction of technetium with green rust. *J. Colloid Interface Sci.*
445 **2003,** *268*, 408-412.
446 11. Jaisi, D. P.; Dong, H. L.; Plymale, A. E.; Fredrickson, J. K.; Zachara, J. M.;
447 Heald, S. C.; Liu, C., Reduction and long-term immobilization of technetium by Fe(II)
448 associated with clay mineral nontronite. *Chem. Geol.* **2009,** *264*, 127-138.
449 12. Peretyazhko, T.; Zachara, J. M.; Heald, S. C.; Kukkadapu, R. K.; Liu, C.;
450 Plymale, A. E.; Resch, C. T., Reduction of Tc(VII) and Fe(II) sorbed on Al (hydr)oxides.
451 *Environ. Sci. Technol.* **2008,** *42*, 5499-5506.
452 13. Cui, D.; Eriksen, T. E., Reduction of pertechnetate in solution by heterogeneous
453 electronic transfer from Fe(II) containing geological material. *Environ. Sci. Technol.*
454 **1996,** *30*, 2263-2269.
455 14. Yang, H.; Lu, R.; Downs, R. T.; Costin, G., Goethite, α-FeO(OH), from single-
456 crystal data. *Acta Crystallographica Section E* **2006,** *E62*, 250-252.
457 15. Schwertmann, U.; Cornell, R. M., *Iron oxides in the laboratory. 2nd Edition*.
458 WILEY-VCH: Weinheim, 2000.
459 16. Gibbs, C. R., Characterization and application of ferrozine iron reagent as a
460 ferrous indicator. *Anal. Chem.* **1976,** *48(8)*, 1197-1201.
461 17. Um, W.; Chang, H.; Icenhower, J. P.; Qafoku, N.; Serne, R. J.; Smith, S. C.;
462 Buck, E. C.; Kukkadapu, R. K.; Bowden, M. E.; Westsik Jr., J. H.; Lukens, W. W.

Immobilization and limited reoxidation of Technetium-99 by Fe(II)-goethite; PNNL-19833; Pacific Northwest National Laboratory: Richland, 2010.
18. Um, W.; Serne, R. N.; Krupka, K. M., Surface complexation modeling of U(VI) sorption to Hanford sediment with varying geochemical conditions. *Environ. Sci. Technol.* **2007,** *41(10)*, 3587-3592.
19. Bacon, D. H.; McGrail, B. P. *Waste form release calculations for the 2001 immobilized low-activity waste performance assessment*; PNNL-13369; Pacific Northwest National Laboratory: Richland, WA, 2001.
20. Newville, M., IFFEFIT: interactive XAFS analysis and FEFF fitting. *J. Synchrotron Radiat.* **2001,** *8*, 322-324.
21. Ravel, B.; Newville, M., ATHENA, ARTEMIS, HEPHAESTUS: data analysis for X-ray absorption spectroscopy using IFEFFIT. *J. Synchrotron Radiat.* **2005,** *12*, 537-541.
22. Lukens, W. W.; Bucher, J. J.; Edelstein, N. M.; Shuh, D. K., Products of pertechnetate radiolysis in highly alkaline solution: Structure of $TcO_2 \cdot xH_2O$. *Environ. Sci. Technol.* **2002,** *36*, 1124-1129.
23. Schwertmann, U., Solubility and dissolution of iron oxides. *Plant Soil* **1991,** *130*, 1-25.
24. Langmuir, D., *Aqueous environmental geochemistry*. Prentice Hall: Upper Saddle River, New Jersey, 1997.
25. Peretyazhko, T.; Zachara, J. M.; Heald, S. M.; Jeon, B.-H.; Kukkadapu, R. K.; Liu, C.; Moore, D. A.; Resch, C. T., Heterogeneous reduction of Tc(VII) by Fe(II) at the solid-water interface. *Geochim. Cosmochim. Acta* **2009,** *72*, 1521-1539.
26. He, Y. T.; Traina, S. J., Transformation of magnetite to goethite under alkaline pH conditions. *Clay Minerals* **2007,** *42(1)*, 13-19.
27. Mahoney, L. A.; Russell, R. L. *Vitrification offgas caustic scrubber secondary waste simulant formulation*; PNNL-14582 Rev.1; Pacific Northwest National Laboratory: Richland, 2004.
28. Downward, L.; Booth, C. H.; Lukens, W. W.; Bridges, F. In *A variation of the F-test for determining statistical relevance of particular parameters in EXAFS fits*, 13th International Conference on X-ray Absorption Fine Structure, Stanford, CA, USA, July 9-14, 2006; 2006; pp 129-131.
29. Szytulstroka, A.; Burewicz, A.; Dimitrijevicacute, Z.; Krasacutenicki, S.; Rzdotany, H.; Todorovicacute, J.; Wanic, A.; Wolski, W., Neutron diffraction studies of alpha-FeOOH. *Phys. Status Solidi B.* **1968,** *26(2)*, 429-434.

506 Table 1. Composition of Hanford Tank Waste Treatment and Immobilization Plant

507 Secondary Waste Simulant.

508

Components	Simulant SSS-1 (moles/L)[27]	Simulant SSS-2 (moles/L) Caustic Scrubber Solution; Median Values from [17]
Na	1.8	2.0
Al	NI	1.88E-01
Cr	NI	4.06E-04
Ag	NI	1.25E-05
Cd	NI	3.14E-06
I	NI	9.14E-06
Hg	NI	2.26E-05
Pb	NI	1.80E-05
NH_4^+	1.84	NI
CO_3^{2-}	8.10E-01	4.56E-02
NO_3^-	1.60E-02	6.56E-01
OH^-	1.92	7.96E-01
PO_4^{3-}	NI	1.37E-02
SO_4^{2-}	NI	8.82E-03
TOC (as acetate)	7.80E-02	NI
TOC (as oxalate)	NI	1.88E-01

NI = not included; TOC = total organic carbon.

509
510

511 Table 2. Summary of Tc-goethite preparation methods and Tc removal efficiencies.
512

Test Description and Tc Removal	Samples[a]						
	2	**2-1**	**2-2**	**2-3**	**2-3*[b]**	**2-4**	**2-5**
Additional Fe(III) armoring	Yes	Yes	No	No	No	Yes	Yes
Initial solution[c]	DIW	DIW	DIW	SSS-1	SSS-2	SSS-1	DIW
Initial goethite mass (g)	3.47	2.75	2.75	2.75	2.0	2.75	2.75
Initial pH	1.78	1.47	1.47	1.47	1.58	1.47	1.47
pH after 1 day reaction with Fe(II)	2.25	2.06	2.04	2.04	1.98	2.03	3.54
pH after Tc spike	2.01	2.06	2.04	13.0	13.5	13.0	3.03
Initial spiked-Tc mass (μg)	597	551	501	522	5547	546	615
Reaction time with Tc	1 day	2 days	2 days	2 days	1 day	2 days	2 days
Adjusted pH by NaOH before Fe(III) addition	NA	NA	NA	NA	13.5	NA	13.3
pH after mixing Fe(III) and NaOH	13.0	13.3	13.3[d]	13.0[d]	13.4	13.0[d]	13.3
Reaction time in oven (day)	7 day	7 day	7 day	7 day	7 day	7 day	7 day
Final pH after heating in oven	12.9	13.3	13.3	13.0	13.3	13.3	13.4
Final solid mass (g)	6.53	6.05	3.24	3.51	5.10	6.43	6.41
Final Tc removal on solid (μg/g)[e]	85.7	84.4	149.1	143.1	1020	78.9	96.0
Tc uptake in goethite (%)	**93.7**	**92.7**	**96.5**	**96.3**	**93.8**	**92.9**	**100.0**
XAFS sample collection	NSLS	NA	SSRL	NA	SSRL	NA	SSRL

(a) "No Fe(III)" indicates no armoring process was conducted with additional Fe(III) for Samples 2-2 and 2-3. NA indicates "not applicable"; NSLS = National Synchrotron Light

Source; SSRL = Stanford Synchrotron Radiation Laboratory. XAFS = x-ray absorption fine structure (spectroscopy).

(b) Additional Tc-goethite sample, Sample 2-3*, was prepared in simulant (SSS-2) with a high Tc concentration, 4.2×10^{-4} M and 0.1M of Fe(II).

(c) The initial solutions = deionized (DI) water, synthetic scrubber solution (SSS-1) or (SSS-2) refer to Table SI-1 for compositions.

(d) The pH values were measured after addition of NaOH in Samples.

(e) The final concentration of Tc on Tc-goethite was determined by acid digestion.

513

514

515

516

517

518

519

520 Table 3. Structural parameters of Tc derived from EXAFS analysis.

Samples	Neighbor atoms	CN	R(Å)	σ^2	ΔE_0	p(F)
Tc-goethite Sample 2 (R-factor = 0.006)	O	6	2.017(5)	0.0023(3)	0(1)	<0.001
	Fe	4	3.074(8)	0.0064(6)	0(1)	<0.001
	Fe	4	3.52(2)	0.0064(6)[b]	0(1)	<0.001
	Tc	0.5(2)	2.51(2)	0.0064(6)[b]	0(1)	0.046
Tc-goethite Sample 2-2 (R-factor = 0.011)	O	6	2.020(6)	0.0040(4)	-2(1)	<0.001
	Fe	4	3.09(1)	0.0084(7)	-2(1)	<0.001
	Fe	4	3.53(1)	0.0084(7)[b]	-2(1)	<0.001
Tc-goethite Sample 2-3 (R-factor = 0.033)	O	6	2.014(8)	0.0049(5)	-3(2)	<0.001
	Fe	4	3.08(2)	0.013(2)	-3(2)	<0.001
	Fe	4	3.54(2)	0.008(1)	-3(2)	<0.001
Tc-goethite Sample 2-5 (R-factor = 0.037)	O	6	2.02(1)	0.0060(6)	-2(1)	<0.001
	Fe	4	3.10(2)	0.009(1)	-2(1)	<0.001
	Fe	4	3.53(5)	0.017(6)	-2(1)	0.25
Goethite[‡]	O	6	1.95-2.09			
	Fe	2	3.01			
	O	1	3.23			
	Fe	2	3.28			
	Fe	4	3.59			

521 * S_o^2=1.0; coordination number (CN); interatomic distance (R); disorder parameter
522 (σ^2); energy shift (ΔE_0); goodness of fit parameter (R-factor); F-test [p(F)]. A F-test was
523 performed on each scattering shell to determine the best model**.** If the probability of
524 F[p(F)] is less than 0.05, the addition of that shell improves the fit to greater than 2σ and
525 that shell was considered to be observed in the experiment. More details for F-test is
526 referred to Downward et al. [28]. [‡] Goethite from Szytulstroka et al. [29].
527

528 **Figure captions.**

529

530 Figure 1. X-ray diffraction patterns for initial goethite and final Tc-goethite solids.
531 Arrows (red) indicate presence of magnetite. Sample 2-3* was prepared in simulant SSS-
532 2 with high Tc(VII) concentration, 4.2×10^{-4} M and 0.1 M Fe(II) without additional
533 armoring.

534

535 Figure 2. SEM images for Tc-goethite samples (a) initial goethite; (b) final Tc-goethite
536 Sample 2-2; (c) final Tc-goethite Sample 2-5; (d) final Tc-goethite Sample 2-3*; (e) EDX
537 for Tc-goethite Sample 2-3* prepared using simulant-2 (caustic scrubber median) with
538 high Tc concentration and 0.1 M of Fe(II) without additional armoring process. A beam
539 location is a cubic-shaped particle described as a pink rectangle denoted as "Fe particle"
540 in Figure 2d.

541

542 Figure 3. TEM images for Tc-goethite samples: (A) high magnification image of Tc-
543 goethite Sample 2-2; (B) presence of visible magnetite with goethite in agreement with
544 XRD in Sample 2-2; (C) electron diffraction pattern taken along the **B**[001] direction of
545 goethite in Sample 2-2; (D) TEM/EDX analysis of Tc in Sample 2-2. The Tc is
546 identified by the L-lines at close to 2.5 keV. The peaks for Si and Cu are artifacts of the
547 sample preparation and the specimen holder, respectively; (E) TEM/EDX analysis of Tc-
548 goethite Sample 2-3* showing trace amount of technetium.

549

Figure 4. Batch leaching results for Tc-goethite samples as a function of reaction time with different pH buffer solutions (4, 7, and 10), IDF pore water, and GL. (a) Tc(tot) leaching for Sample 2; (b) dissolved Fe(tot) for Sample 2; (c) measured pHs for Sample 2; (d) Tc(tot) leaching for Tc-goethite Samples 2, 2-2, and 2-5 in IDF pore water. The leachates were analyzed in triplicate, and the average values were used.

Figure 5. Normalized XANES spectra for Tc(VII) and Tc(IV) standards, and Tc-goethite samples. (a) The black symbol (rectangular) and the solid line in Tc-goethite spectra indicate the measured data and a linear combination fit, respectively for Tc-goethite samples before leaching; (b) The rectangular black symbol and red line in Tc-goethite spectra indicate the measured data and a linear combination fit, respectively for Tc-goethite samples after 180 days leaching. The reacted Sample 2 in air was contacted for 180 days with atmospheric air.

567 Figure 1.

568

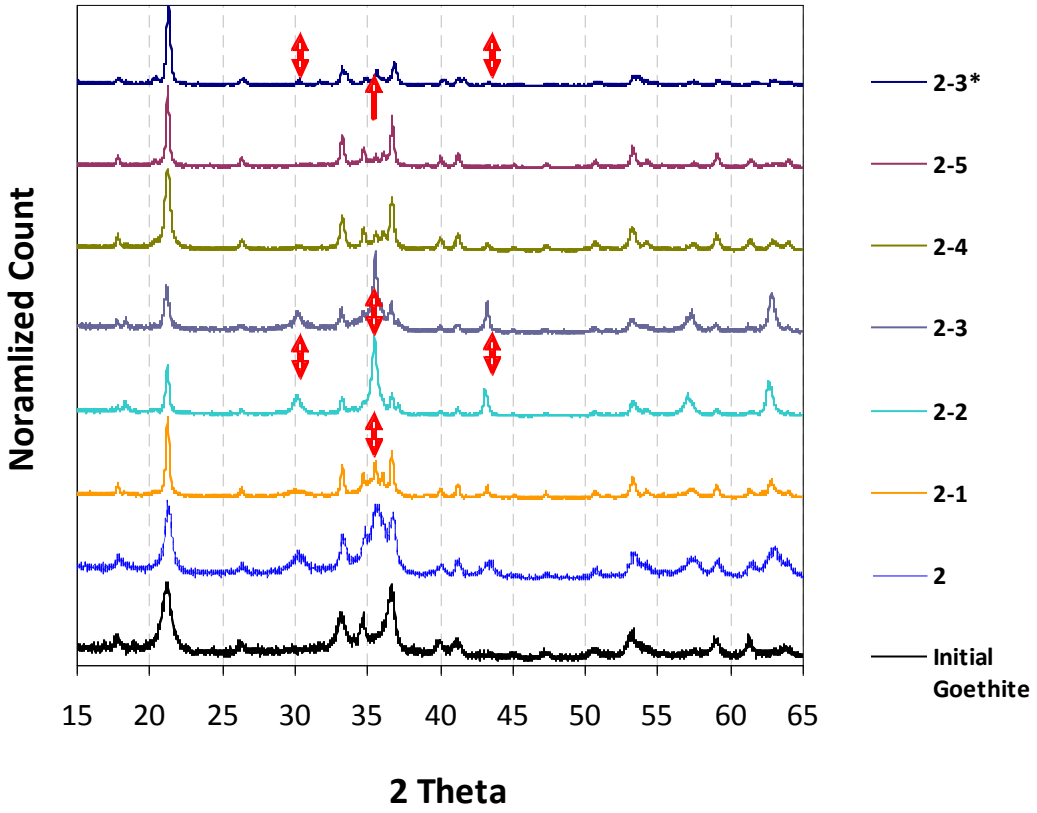

569

570

571
572
573
574
575
576
577
578
579
580
581
582
583
584
585

Figure 2.

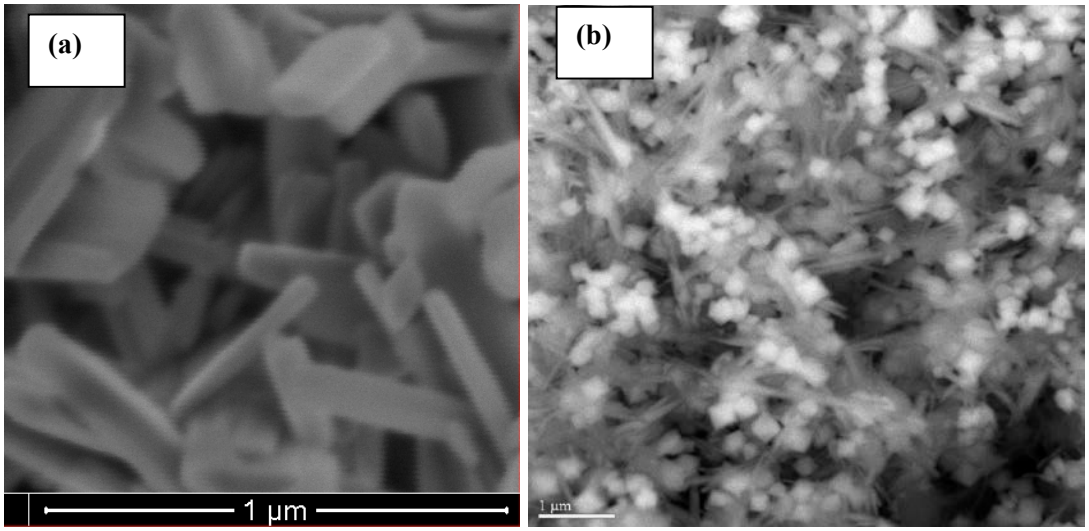
(a)
1 µm
(b)
1 µm

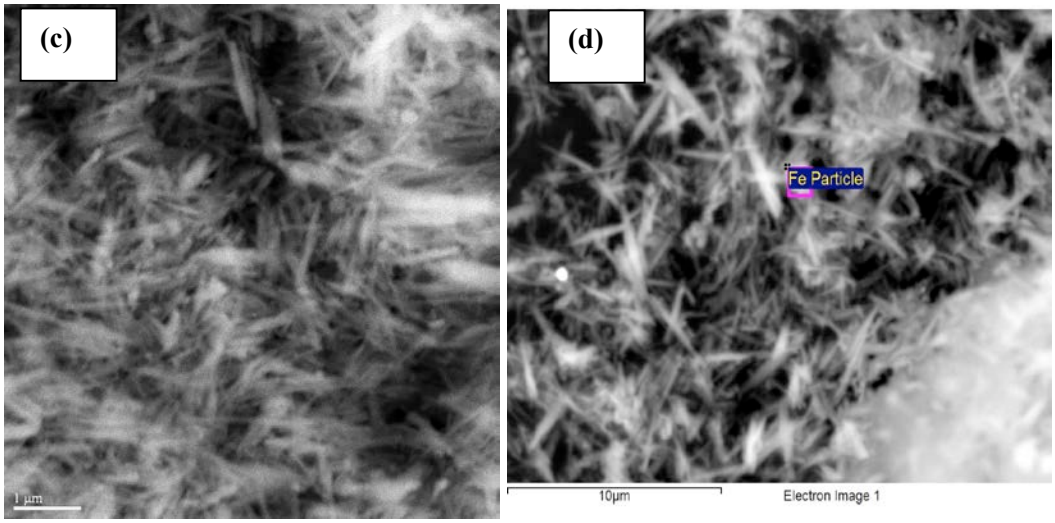
(c)
1 µm
(d)
Fe Particle
10µm
Electron Image 1

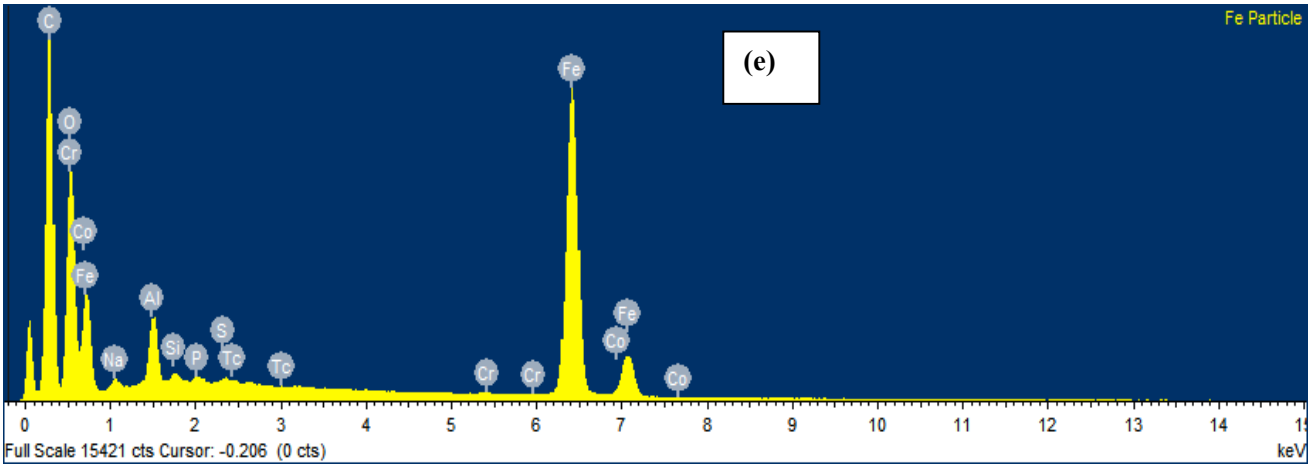
(e)
Fe Particle
C
O
Cr
Co
Fe
Al
Na
Si
P
S
Tc
Tc
Cr
Cr
Fe
Fe
Co
Co
0
1
2
3
4
5
6
7
8
9
10
11
12
13
14
Full Scale 15421 cts Cursor: -0.206 (0 cts)
keV

593 Figure 3.

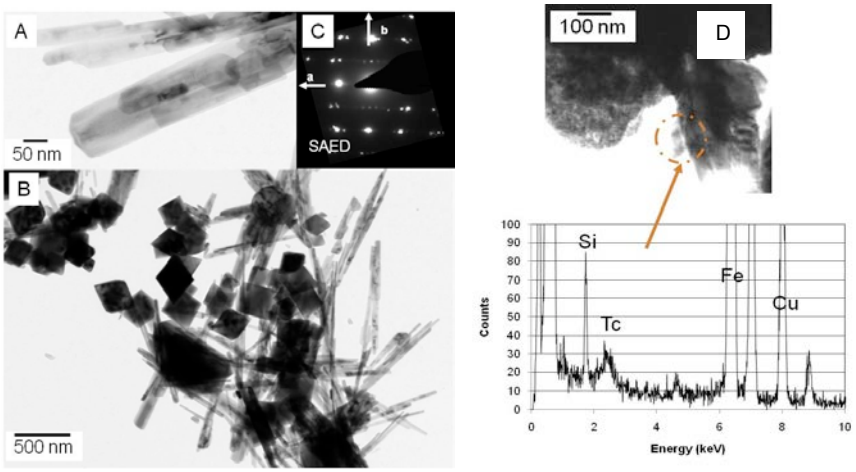

594

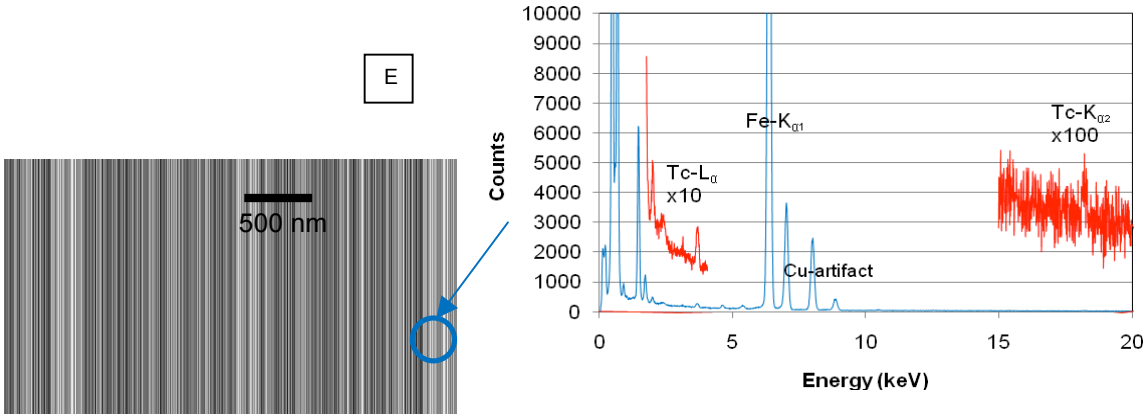

595

596

597

598 Figure 4.

599

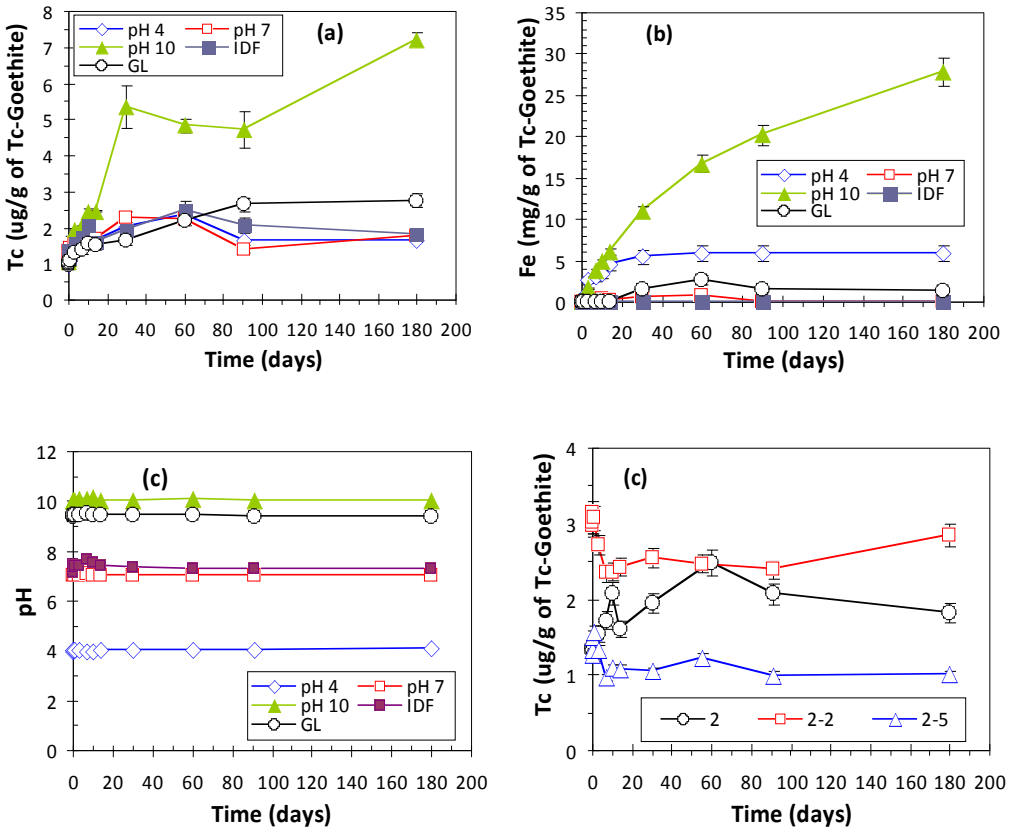

600

601

602

603

604

605

606

607

608

609

610

611

612 Figure 5.

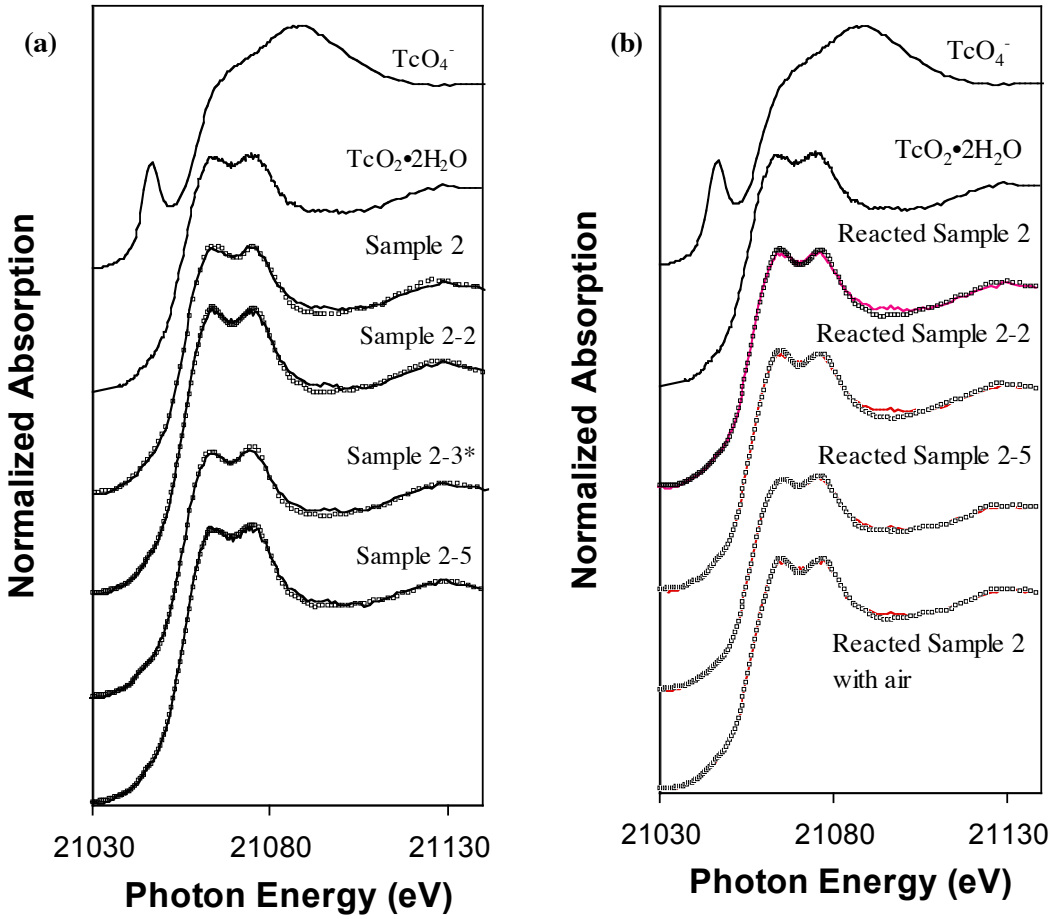

613

614

615

616

Brief: *Fabrication of Fe(II) treated goethite for sequestration of Tc(VII) and limited re-oxidation of Tc(IV) present as coprecipitates within goethite lattice are discussed.*

ACKNOWLEDGEMENT

The authors are grateful to Wayne McKinney and Peter Takacs for very useful discussions. The Advanced Light Source is supported by the Director, Office of Science, Office of Basic Energy Sciences, Material Science Division, of the U.S. Department of Energy under Contract No. DE-AC02-05CH11231 at Lawrence Berkeley National Laboratory.

DISCLAIMER